COMPUTATIONAL THERMODYNAMICS STUDY OF THE INFLUENCE OF TUNGSTEN IN SUPERDUPLEX STAINLESS WELD METAL

S. Wessman, L. Karlsson, R. Pettersson and Agneta Östberg

ABSTRACT

Tungsten is used by some duplex stainless steel producers for partial substitution of molybdenum, both elements enhancing the corrosion resistance of duplex stainless steel. The negative aspect of both molybdenum and tungsten alloying is that they increase the tendency to precipitate intermetallic phases, which may have a detrimental effect on corrosion and mechanical properties. The temperature region for intermetallic phase precipitation is about 700-1000 °C, depending on alloy composition, and the time for precipitation is within minutes for superduplex steels.There has been scientific discussion on the relative effects of Mo alone or Mo-W on intermetallic precipitation behaviour in superduplex steels for the past two decades. While the base material response to ageing and precipitation of intermetallic phases has been satisfactorily assessed, weld metal has proved more of a challenge. The main reason for this is that welding is a very complex process introducing many parameters to the assessment which not have to be considered in studies of base material. For example superduplex weld metal typically solidify fully ferritic but may in case excessive nitrogen is added solidify as a mixture of ferrite and austenite. The solidification mode may vary also between weld passes as a consequence of minor variations in composition. Ferritic solidification is the preferred mode, giving the well known Widmanstätten austenite, which forms in the solid state during cooling. Mixed mode solidification gives a vermicular appearance, which is known to increases the tendency to intermetallic formation. A comprehensive study using computational thermodynamics was done to investigate this matter. This study included equilibrium calculations, Scheil-Gulliver solidification simulations, and calculations of the driving force for intermetallic phase precipitation and further a study of diffusion of Mo and W in these alloy systems. The different approaches were applied on model superduplex weld metals with nominal compositions matching commercial superduplex fillers available today. The principal conclusion is that all thermodynamic calculations clearly indicates the W containing filler to show a more pronounced sensitivity to heat treatments by precipitation of intermetallic phases.

IIW-Thesaurus keywords: Computation; Thermodynamics; Calculation; Duplex stainless steel; Weld metal.

1 Introduction

The corrosion resistance of a duplex stainless steel is mainly depending on the alloying level of the elements chromium, molybdenum and nitrogen, and tungsten added by some steel producers. Chromium levels are usually about 20-30%, molybdenum varies from none in lean duplex up to about 4% in superduplex, nitrogen about 0.1 to 0.4% and tungsten from none up to about 2%. The additions are guided by the desired corrosion resistance and mechanical properties and balanced to give a phase balance of about 50/50 ferrite and austenite. The steel composition is also limited by the fact that higher levels of Cr, Mo and W promote the precipitation of deleterious intermetallic phases. Higher levels i.e. higher alloyed superduplex steels require more cautious heat treatments compared to more robust lean steels due to risk of precipitation of property-impairing phases.

Nitrogen is an important alloying element in modern duplex stainless steels and its introduction established the good austenite reformation in the heat affected zone (HAZ) which is vital for successful use of duplex grades [1]. Nitrogen is an austenite former, supporting the nickel, and it is often also added to the shielding gas in order to compensate for losses from the weld pool [2]. The desired microstructure morphology of duplex weld metal is denoted Widmanstätten with the matrix phase ferrite nicely decorated with the austenite precipitating in an angular web pattern. If, however, the balance between austenite and ferrite forming elements, for example through addition of nitrogen, exceeds a critical limit the solidification will turn to an undesirable mixed mode. This solidification mode results in a microstructure dominated by the austenitic phase with a typical vermicular appearance [3]. Since this mode tends to give a ferrite enriched with Cr, Mo and W, it is also prone to precipitate intermetallic phases. Typical microstructures of both solidification modes are given in Figure 1.

Doc. IIW-2293 recommended for publication by Commission IX "Behaviour of Metals Subjected to Welding".

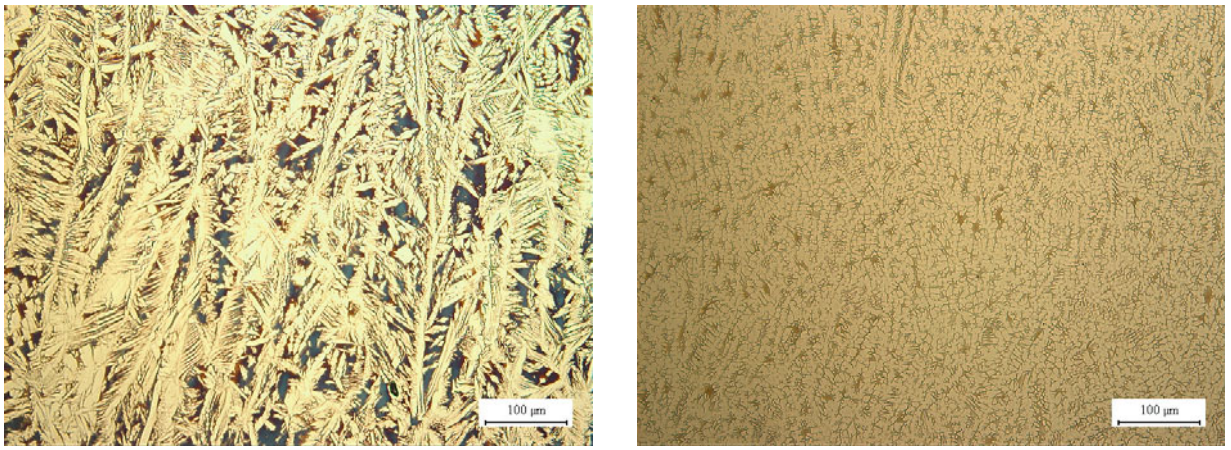

Figure 1 – Typical Widmanstätten (l.) and mixed mode solidification (r.) microstructures, both 25Cr superduplex weld metal

There is a refreshing tradition of academic discussions between advocators of Mo [4-6] and the opponents [7-10] with allegiance to Mo-W as alloying strategies for superduplex stainless steels. The scientific basis for the discussion is precipitation of sigma phase contra precipitation of chi phase. It is well known that sigma phase is difficult to precipitate but grows rapidly, for chi phase it is vice versa. The explanation given by Nilsson *et al.* [4] is that due to the tetragonal structure of the sigma phase there is a large mismatch with the ferritic matrix. Precipitation thus leads to large coherency strains and is relatively difficult. The cubic chi phase is, however, not obstructed by this and therefore precipitates more swiftly. Chi phase also precipitates at somewhat lower temperature than sigma phase [11]. Both sigma and chi phase have a strongly detrimental effect on the impact toughness and decrease the corrosion properties [12] Since the levels of precipitation required to degrade properties are very low, impact toughness testing is the most appropriate tool to detect precipitation. Standard metallographical work and SEM survey are important tools for elucidation but does not offer the same degree of quantitative evaluation. Metallographic evaluation is also complicated by the fact that the properties of precipitate structures depend on thermal history and the short times make this a complicated non-equilibrium situation, often with multiple passes as studied by Nishimoto *et al.* [13].

The aim of this work was to evaluate the influence of tungsten in superduplex weld metal on precipitation of intermetallic phases using computational thermodynamics.

2 Approach

This paper presents no experimental results but is an evaluation using computational thermodynamics. An excellent and thorough description of this field of science is given by Lukas *et al.* [14]. The core of approach is a database consisting of multiple assessments of binary, ternary and quaternary alloys, and in some cases also higher order systems, with focus on systems of importance for alloy development. The data is compiled from literature surveys of available experimental information, deciding whether this is reliable or not, and by critical experiments to obtain critical data. The thermodynamic data is stored as Gibbs energy expressions describing each phase, a progressive work involving continuous reassessments and refinement. The assessments are done by complicated multivariable optimisations of thermodynamic parameters in order to fit to the selected experimental results and the output are descriptions of the Gibbs energy of these systems, which make it possible to perform equilibrium calculations. This is a tedious work that requires skilful judgement, since the descriptions must be consistent in higher order systems. The equilibrium is represented by the minimum Gibbs energy and this is assessed by calculations of the phases involved in the system. A common approach is the Calphad (CALculation of PHAse Diagrams) technique, an international approach to collect and describe the thermodynamics of a system [15-17]. With reliable description of existing experimental data, the Calphad method, when correctly done, allows for prediction of multi-component systems where no experimental data are available [18-19].

The software Thermo-Calc version R [20] with the TCFE5 database was used for all calculations, including the Scheil-Gulliver solidification simulations [21-22]. Typical compositions were used in the predictive calculations in order to reduce the influence of irrelevant parameters, and one low-N and one high-N variant were also assessed. The compositions are given in Table 1 and represent two typical superduplex weld metals, a 2507 variant denoted Mo with only Mo and one tungsten alloyed denoted MoW. As the table shows there are differences in Si, Ni, Mo, W and Cu contents, the major difference though being the tungsten content. The validity for the TCFE5 database is given as Fe > 50%, Cr < 30%, Ni < 20%, Mo < 10%, W < 15%, Cu <2% and N <1%. The compositions in Table 1 are thus well within the valid range. A comparison with TCFE5 and long-term heat treated duplex and superduplex steels, held for 6 months at 700-1000 °C,

Table 1 – Compositions used for thermodynamic calculations, [wt-%]

	C	Si	Mn	Cr	Ni	Mo	W	Cu	N
Mo-0.2N	0.015	0.40	0.40	25.00	9.50	4.00	0.01	0.10	0.20
Mo-0.3N	0.015	0.40	0.40	25.00	9.50	4.00	0.01	0.10	0.30
MoW-0.2N	0.015	0.30	0.40	25.00	9.00	3.00	2.00	0.40	0.20
MoW-0.3N	0.015	0.30	0.40	25.00	9.00	3.00	2.00	0.40	0.30

indicate that the database output is in good accordance with experimental results [23]. Additionally, calculations of the tracer diffusion coefficient for molybdenum and tungsten were done using the Dictra version 24 [24] with TCFE5 and TCS Alloys Mobility Database v1.

3 Thermodynamic calculations

The results comprise some different approaches: equilibrium calculations, Scheil-Gulliver solidification simulation, calculation of the driving force for sigma and chi phase precipitation and combinations of Scheil-Gulliver simulations and driving force calculations.

3.1 Equilibrium calculations

A first approach was to calculate the equilibrium microstructure and in Figure 2 the results for the Mo and the MoW alloy with 0.3N are given.

These results give an overview of the equilibrium status for each alloy and nitrogen level. Thermo-Calc suggests a mixed solidification, experience however, is that this is an exception due to excess nitrogen. Some information about the differences in tendency to precipitate intermetallic phases can be seen to the far left in the figures if the amount sigma and chi phase is summarised. At 700°C is the sum sigma + chi about 10% larger for the MoW alloy than the Mo alloy, 29.4% + 3.8% versus 26.8% + 10.0%. Both phases do also precipitate at higher temperature for the MoW alloy. If mole percent is used instead of wt-% the sum for available Mo and W atoms is similar in both alloys. For the Mo alloy the sum is 2.3% and the MoW alloy 1.7 + 0.6, i.e. also 2.3 mole-%.

3.2 Scheil simulation

The next approach is to apply the Scheil-Gulliver solidification simulation, which describes solute redistribution during solidification of an alloy, included as a separate module in Thermo-Calc. This approximates non-equilibrium solidification by assuming a local equilibrium of the advancing solidification front at the solid/liquid interface. These simulations give the information that these alloys solidify with ferrite as primary phase and that austenite precipitates during the continued solidification sequence. Some strange phenomena occur at the very end of the solidification sequence, with nitride and supposedly also sigma phase precipitating from the melt, but this is considered to be an artefact and therefore not further discussed here. It can be noticed that the solidification interval from equilibrium calculations is between 1450-1350 °C but for Scheil simulation between 1450-1250 °C. However, for the Scheil simulation 75% solid phase has formed at about 1370 °C and 90% at about 1350 °C, the solidification for the last 10% thus extends over a 100 °C

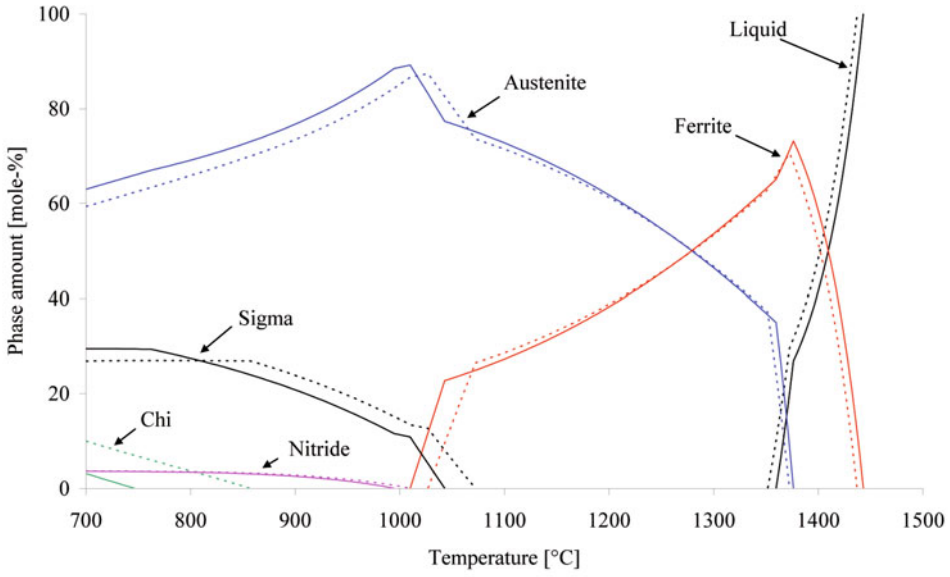

Figure 2 – Phase amount [mole-%] versus temperature [°C] for the Mo with 0.3N (solid lines) and MoW with 0.3N (broken lines)

temperature range. Information about the tendency to form intermetallic phases from the Scheil simulations can be obtained by plotting the chromium, molybdenum and tungsten (for the MoW alloy) content of ferrite, austenite and liquid phase versus temperature. The results are shown below in Figure 3 for alloy Mo and in Figure 4 for alloy MoW. The solidus temperatures from the respective equilibrium calculations are given as horizontal lines.

These simulations indicate clearly that there occurs a slight decrease in alloy content in the ferrite, from the initial 25Cr-4Mo, which progresses until austenite starts to form. This leads to a major increase in Cr (up to 32-35%), Mo (5-8%) and W (4-6%) in final 10% of the melt. This is an indication that during the initial ferritic solidification, the ferrite stabilisers Cr and Mo are preferentially enriched in the growing ferrite. The start of peritectic (ferrite plus austenite) solidification shifts the segregation pattern markedly and there is a drastic increase in potential intermetallic phase formers in the interdendritic areas. Tungsten differs from Cr and Mo by continuously segregating towards the liquid, not towards the initial ferritic phase.

3.3 Calculation of the driving force

The following approach was to apply the concept of calculating the driving force D, which is a thermodynamic quantity [25] defining equilibrium as D = 0. The driving force can be calculated with Thermo-Calc for sigma and chi phase precipitation. This was done by setting all phases except ferrite and austenite as dormant, and, thus assess D-values for precipitation of intermetallic phases.

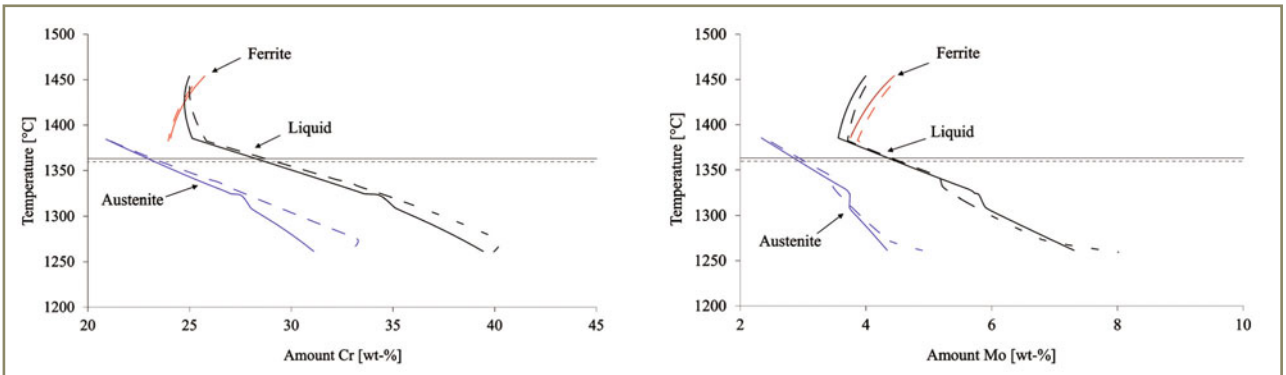

Figure 3 – Mo alloy Scheil simulation with amount Cr (l.) and Mo (r.) in liquid, ferrite and austenite vs. temperature for 0.2N (solid lines) and 0.3N (broken lines). Horizontal lines are solidus temperatures from equilibrium calculations

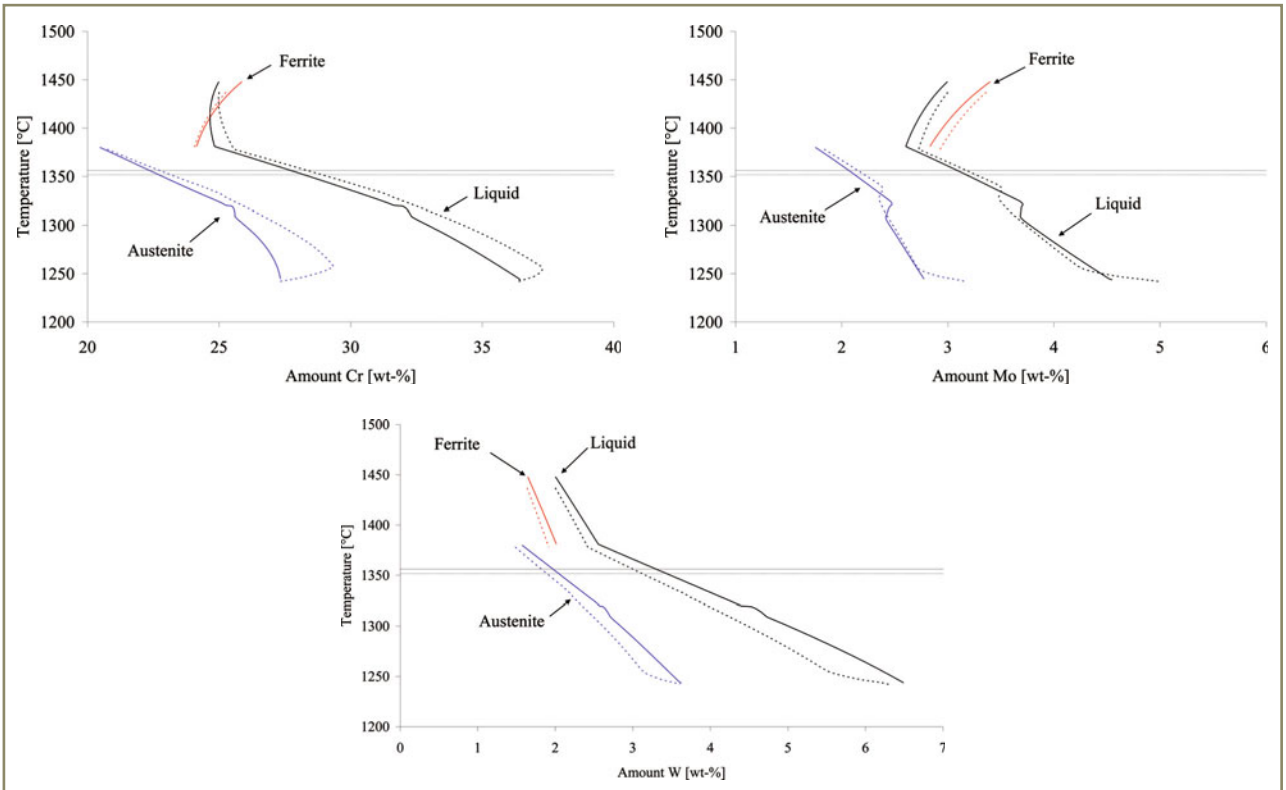

Figure 4 – MoW alloy Scheil simulation with amount Cr (top l.), Mo (top r.) and W (l.) in liquid, ferrite and austenite vs. temperature for 0.2N (solid lines) and 0.3N (broken lines). Horizontal lines are solidus temperatures from equilibrium calculations

A larger value of D indicates a larger tendency for precipitation of respective phase. The calculations were made in two-steps with first an equilibrium calculation at 1100 °C in order to obtain the ferrite composition. This was followed by a calculation at 900 °C for D(sigma) and D(chi) with respective typical ferrite compositions. The reason for this approach is that it is the ferrite which decomposes to intermetallic phases and the ferrite composition is determined by the annealing temperature, usually ~1100 °C for superduplex steels, hence the two-step procedure. The results are presented in Figure 5 with driving force and ferrite amount versus nitrogen content. The ferrite content is included in order to demonstrate the immense effect of nitrogen on ferrite/austenite phase balance.

The results in Figure 5 indicate that for both alloys there is an increasing tendency for intermetallic phase formation with increasing nitrogen content. This might sound a bit confusing compared to literature since it is well known that nitrogen suppresses intermetallic phase precipitation [26]. As was shown by Hertzman *et al.* [6] this is, however, only truly valid for austenitic steels, while in duplex steel the effect of nitrogen per se is only slight but altering the phase balance is the major effect. What Figure 5 shows is in fact the segregation of ferrite stabilisers Cr, Mo and W to the shrinking ferrite. Since these elements all are intermetallic formers, D(sigma) and D(chi) increase with increasing nitrogen content. The difference in austenite/ferrite balance at 1100 °C is negligible but the tendency to form intermetallic phases is larger for the MoW alloy than for the Mo alloy. There is also a difference in that for the Mo alloy sigma phase is the primary phase with a larger driving force, while in the MoW alloy there is a larger driving force for chi phase precipitation.

3.4 Driving force after Scheil simulation

The above approach is however somewhat limited due to the fact that it is more appropriate for base material calculations. A combination of Scheil simulation and driving force calculation was therefore tried. From a Scheil simulation the Cr, Ni, Mo, N and W contents of the ferrite (W only for the MoW alloy) were selected at solid contents from 5 to 95%. These compositions were then used in a driving force calculation for sigma and chi phase, done at 900 °C. The results are presented below in Figure 6 for

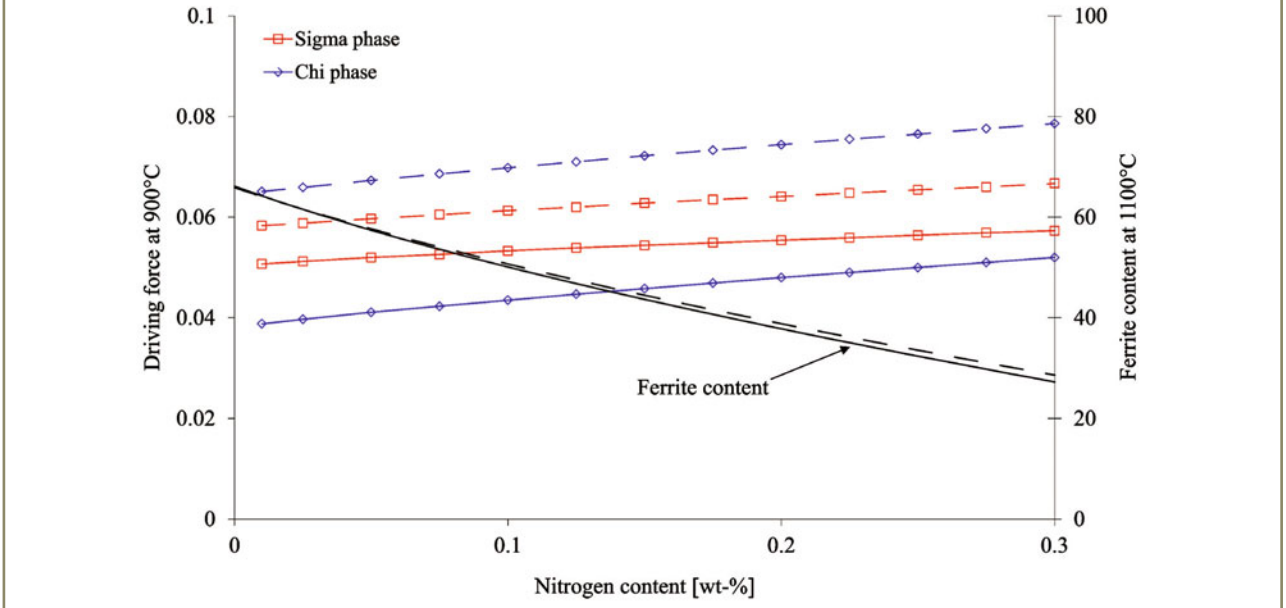

Figure 5 – Driving force for sigma and chi phase for the Mo alloy (solid lines) and the MoW alloy (broken lines) at 900 °C and also ferrite content [mole-%] at 1100 °C versus nitrogen content [wt-%]

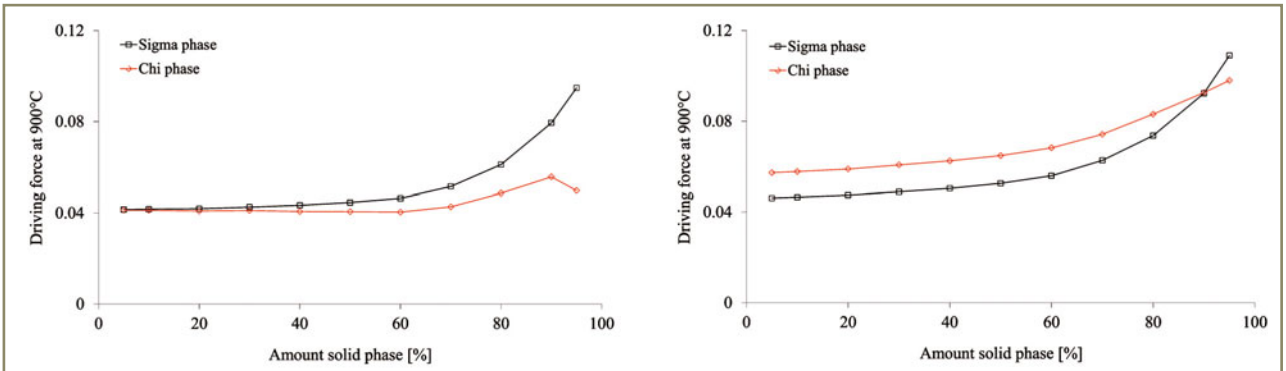

Figure 6 – Driving force for sigma and chi phase formation for the Mo alloy (l.) and MoW alloy with 0.3N (r.) at 900 °C

the Mo and MoW alloy. In order to simplify the calculations, the compositions for C, Si, Mn, Cu and W (for the Mo alloy only) used are those of the ferrite at 1100 °C.

The observations from these calculations are that the shift between sigma and chi phase is the same as in Figure 5 for the alloys. Both alloys also show an increasing tendency for intermetallic phase formation with increasing solid content, for the Mo alloy the increase occurs above 60% solid phase, while for the MoW alloy there is a more steady continuous increase. The MoW alloy also has higher absolute values of driving force indicating a larger tendency to intermetallic phase formation. An interesting observation is that there is no difference in driving force between 0.2N and 0.3N, neither for the Mo alloy nor for the MoW alloy. This is probably due to the fact that ferrite is a poor nitrogen solvent and the major effect, as shown in Figure 5, is on the ferrite/austenite phase balance. One could have expected, however, a different shift between 0.2N and 0.3N, when solidification turns from liq → ferrite to liq → ferrite + austenite, but nitrogen suppresses the liquidus and this shift is at about the same temperature.

3.5 Scheil simulation with ferrite suspended

In order to increase the understanding of the undesired mixed mode solidification, the ferrite phase was suspended from the calculations. Unfortunately the Scheil module in Thermo-Calc does not allow for only setting this phase dormant, i.e. values are calculated for the phase but it is not allowed to precipitate. The results are unsurprising since if something is removed then something else will emerge and in this case eventually sigma phase will appear. It is interesting that this occurs at a higher temperature, i.e. earlier, for the 0.2N alloy. This is, of course, the response nitrogen will give in an austenitic alloy, which the suspension of ferrite has led to. Segregation of the main elements is given in Figure 7 for the Mo alloy and in Figure 8 for the MoW alloy.

The segregation results should be compared with the results in Figure 3 for the Mo alloy and in Figure 4 for the MoW alloy, where ferrite is included in the calculations. The deviation for the Mo alloy is that the Cr segregation to the melt is more pronounced. There is also an expected segregation of Mo from the melt towards sigma phase as soon as it is formed. The same results are seen for the MoW alloy, where tungsten exhibits the same pattern as Mo. The little "hook" at end of the 0.3N graphs is a result of nitride formation.

3.6 Driving force after Scheil simulation with ferrite suspended

The last alternative was to pick compositions of the liquid at certain points of the Scheil simulation with ferrite suspended and then to use these in a driving force calculation. In order to simplify the calculations, new compositions were only used for Cr, Ni, Mo, W (the MoW alloy only) and N, with other elements according to Table 1. All phases except liquid and austenite were set dormant and D(sigma) and D(chi) at 900 °C was assessed, as previously. The calculations were done only during the part of solidification at which austenite was precipitated, since the sigma phase interval is assumed irrelevant to this approach. The results are presented in Figure 9 for the Mo and MoW alloy with 0.3N with driving force for sigma and chi phase versus amount solid phase.

The results from this approach end up with the same conclusion as in Figure 6, the later part of solidification giving rise to a liquid with a pronounced tendency to form intermetallic phases.

4 Kinetics and diffusion

There are some open questions about molybdenum and tungsten diffusion in the previous literature section. Kondo *et al.* [7] considered W thermodynamically equivalent but kinetically non-equivalent to Mo with respect to the formation of sigma phase. Lee *et al.* [8] reported diffusion coefficients of $D^{W}_{\alpha\text{-Fe}}=10^{-21}$ m²/s and $D^{Mo}_{\alpha\text{-Fe}}=10^{-14}$ m²/s at 800 °C. The Dictra software comprises a diffusion database with assessments from various systems and tracer diffusion coefficients are given here. In Figure 10

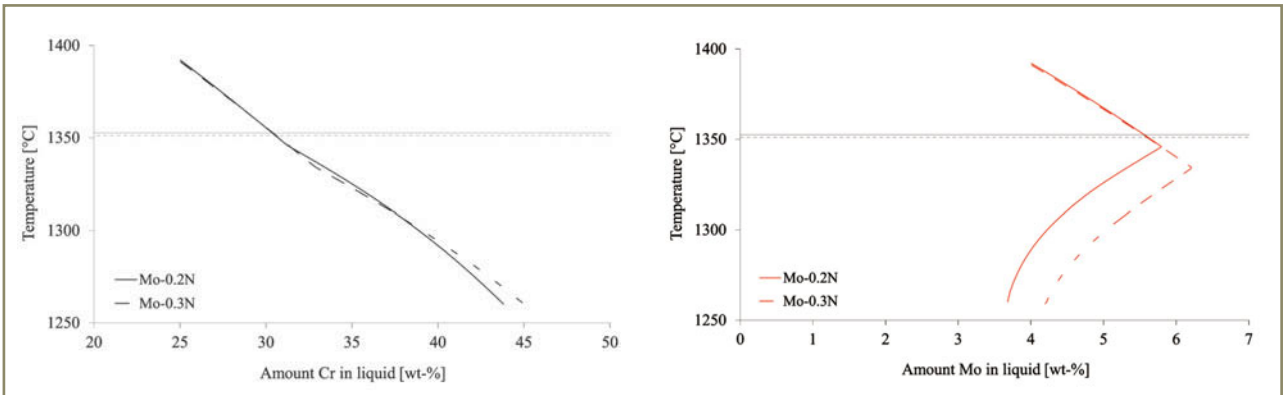

Figure 7 – Scheil simulation with amount Cr (l.) and Mo (r.) in liquid [%] vs. temperature [°C] for the Mo alloy with 0.2N (solid lines) and 0.3N (broken lines), Horizontal lines are solidus temperatures from equilibrium calculations. The ferrite phase is suspended in, both calculations

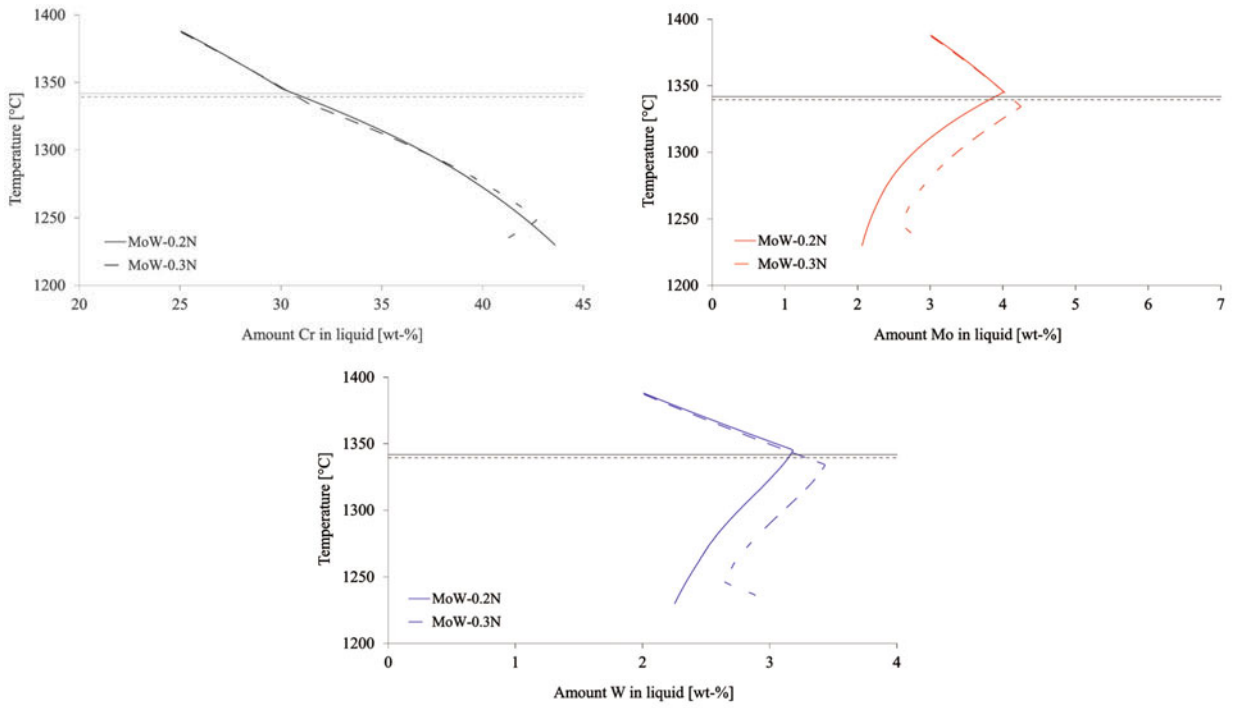

Figure 8 – Scheil simulation with amount Cr (top l.), Mo (top r.) and W (l.) in liquid [%] vs. temperature [°C] for the MoW alloy with 0.2N (solid lines) and 0.3N (broken lines), Horizontal lines are solidus temperatures from equilibrium calculations. The ferrite phase is suspended in both calculations

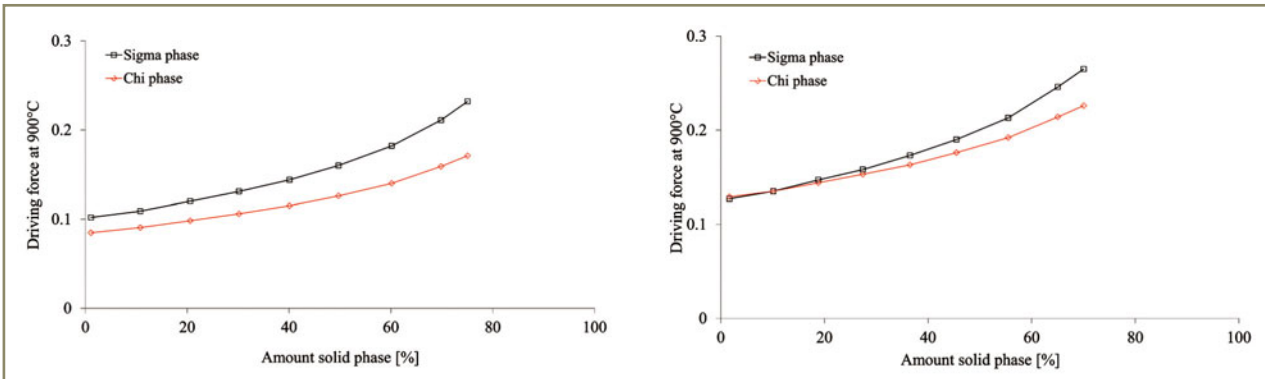

Figure 9 – Driving force for sigma and chi phase for the Mo alloy (l.) and the MoW alloy (r.) at 900 °C, ferrite suspended and 0.3N for both alloys

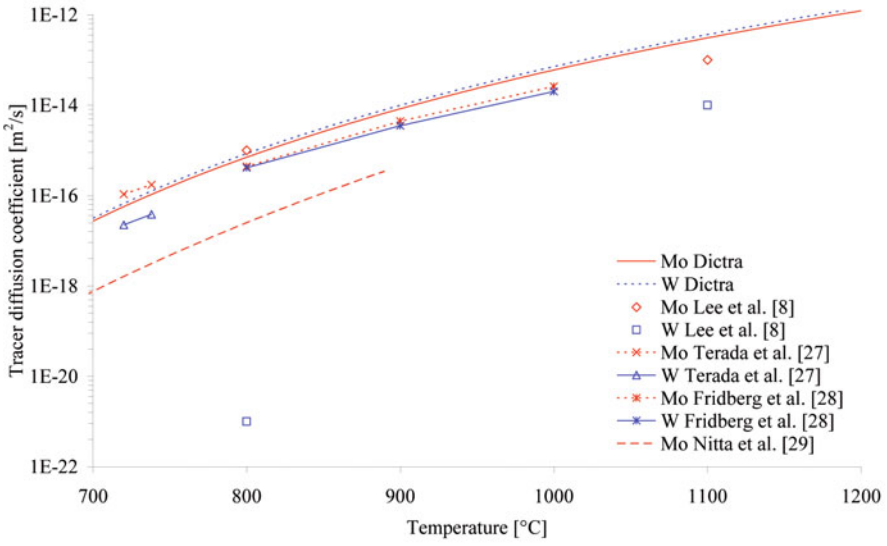

Figure 10 – Diffusion data summary for Mo and W [m²/s] in ferrite phase of iron

the diffusion data for Mo and W in ferrite from Lee *et al.*, Terada *et al.* [27], Fridberg *et al.* [28], Nitta *et al.* [29] and Dictra are summarised. The results indicate that the results from Terada, Fridberg and Dictra are relatively similar. The results for Mo according to Nitta deviate somewhat and for Lee the results for W differ so seriously that they must be considered as erratic. The conclusion must be that if there is a difference in diffusion coefficient between W and Mo in ferrite it is relatively slight, at least in the systems evaluated here. The results also suggest that a more thorough evaluation of the diffusion of Mo and W in high alloyed stainless steels is of interest in order to assess reliable mobilities for these systems.

It has been suggested that the atomic weight (and thus also size) difference between molybdenum (95.94 g/mole) and tungsten (183.85 g/mole) has a significant influence. A useful way to validate this statement is to evaluate the influence of these elements on the lattice spacing. In the handbook of lattice spacings by Pearson [30] such data is available, and it is seen that the difference in lattice spacing for a given atomic-% Mo or W is marginal.

5 Summary and conclusions

Tungsten is used by some duplex stainless steel producers as partial substitution for molybdenum, a practice that has aroused extensive discussions in the materials science world. Many papers have shown that alloying with tungsten gives a more rapid precipitation of intermetallic phases in superduplex base material and consequently a quicker decrease of corrosion and toughness properties [4-6]. The advocators have, naturally, shown the opposite in their papers [7-10]. Applying this concept to weld metal is somewhat more complicated because solidified duplex weld metal can show two modes: a ferrite-dominated microstructure with the austenite present as Widmanstätten precipitates and an austenite-dominated microstructure with austenite present as dendritic or vermicular precipitates.

The thermodynamic simulations, done with Thermo-Calc, were displayed as equilibrium plots, Scheil simulation plots, segregation plots and driving force plots. The effect of a mixed mode solidification, with austenite as the primary phase, was tested by suspending ferrite from the calculations. The calculations were done on model alloys of a Mo- and a Mo and W-containing alloy with two levels of nitrogen content. The results indicate:

– Both alloys solidify with ferrite as the primary phase, with a higher nitrogen content giving an earlier start of austenite formation.

– There is segregation of the intermetallic formers Cr, Mo and W towards the liquid as soon as austenite starts to form, the exception is W which continuously segregates towards the liquid even when only ferrite is precipitated in the melt.

– The segregation of these elements has a clear effect in the driving force calculations and the later solidified matter shows a higher driving force for intermetallic phase precipitation.

– There is also a larger tendency for intermetallic phase formation in the W-alloyed filler than Mo-alloyed, the latter with chi phase as primary phase and the former with sigma phase.

The principal conclusion is that experience from earlier work and all thermodynamic calculations clearly indicates the W containing filler to show a more pronounced sensitivity to heat treatments by precipitation of intermetallic phases.

Acknowledgements

The results assessed within this paper emerge from research financed by Outokumpu Stainless AB, AB Sandvik Materials Technology and ESAB AB within the member programme “Institutet för Metallforskning” at Swerea KIMAB. Greta Lindwall/Swerea KIMAB gave vital support for diffusion data assessments.

References

[1] Hertzman S., Brolund B. and Ferreira P.J.: An experimental and theoretical study of heat-affected zone austenite reformation in three duplex stainless steels, 1997, Met. & Mat. Trans. A, vol. 28, no. 2, pp. 277-285.

[2] Hertzman S., Wessman S., Brorson S. and Liljas M: Wedling of nitrogen alloyed stainless steels – nitrogen balance aspects, 2004, Proc. High Nitrogen steels HNS, Ostend, Belgium, pp. 563-576.

[3] Gregori A. and Nilsson J.-O.: Decomposition of ferrite in commercial superduplex stainless steel weld metals; microstructural transformations above 700 °C, 2002, Met. & Mat. Trans. A, vol. 33, no. 4, pp. 1009-1018.

[4] Nilsson J.-O., Huhtala T., Jonsson P., Karlsson L. and Wilson A.: Structural stability of super duplex stainless weld metals and its dependence on tungsten and copper, 1996, Met. & Mat. Trans. A, vol. 27, no. 8, pp. 2196-2208.

[5] Hertzman S., Huhtala T., Karlsson L., Nilsson J.-O. and Nilsson M., Jargelius-Pettersson R., Wilson A.: Microstructure-property relations of Mo- and W-alloyed super duplex stainless steel weld metals, 1997, Mat. Sci. & Tech., vol. 13, no. 7, pp. 604-613.

[6] Hertzman S., Pettersson R., Frisk K. and Jerwin T.: The relation between alloy composition and kinetics of intermetallic phase formation, Proc. 6th World Duplex Conference, Venice, Italy, 2000, pp. 347-354.

[7] Kondo K., Ueda M., Ogawa K., Okamoto H. and Igarashi M.: Precipitation behaviour of sigma-related phases in 25% chromium based super duplex stainless steels, Proc. Innovation Stainless Steel, Florence, Italy, 1993, vol. 2, pp. 2.191-2.196.

[8] Lee Y.H., Kim K.T., Lee Y.D. and Kim K.Y.: Effects of W substitution on σ and χ phase precipitation and toughness in duplex stainless steels, 1998, Mat. Sci. Tech., vol. 14, no 8, pp. 757-764.

[9] Ahn Y.S. and Kang J.P.: Effect of aging treatments on microstructure and impact properties of tungsten substituted 2205 duplex stainless steel, 2000, Mat. Sci. Tech., vol. 16, no. 4, pp. 382-388.

[10] Okamoto H.: The effect of tungsten and molybdenum on the performance of super duplex stainless steels, 1992, Proc. Applications of Stainless Steel '92, Stockholm, Sweden, vol. 1 pp. 360-369.

[11] Nilsson J.-O., Wilson A., Josefsson B. and Thorvaldsson T.: Relationship between pitting corrosion, touhness and microstructure for isothermally heat treated super duplex stainless steel, 1992, Proc. Applications of Stainless Steel '92, Stockholm, Sweden, vol. 1, pp. 280-289.

[12] Nilsson J.-O. and Wilson A.: Influence of isothermal phase transformations on toughness and pitting corrosion of super duplex stainless steel SAF 2507, 1993, Mat. Sci. Tech., vol. 9, no. 7, pp. 545-554.

[13] Nishimoto K., Saida K. and Katsuyama O.: Prediction of sigma phase precipitation in super duplex stainless weldments, Doc. IIW-1717, 2006, Welding in the World, vol. 50, no. 3/4, pp. 13-28.

[14] Lukas H.L., Fries S.G. and Sundman B.: Computational Thermodynamics, the Calphad Method, Cambridge University Press, 2007.

[15] Hillert M.: Calculation of phase equilibria, ASM Seminar on phase transformations 1968, American Society for Metals, pp. 181-218.

[16] Kaufman L. and Bernstein H.: Computer Calculation of Phase Diagrams with Special Reference to Refractory Materials, Academic Press, NY, USA, 1970.

[17] Saunders N. and Midownik A.P.: Calphad Calculations of Phase Diagrams, a Comprehensive Guide, Pergamon Materials Series, vol. 1, 1998.

[18] Fernández Guillermet A.: Thermodynamic calculation of the Fe-Co-W Phase diagram, 1988, Z. Metallkunde, vol. 79, pp. 633-642.

[19] Fernández Guillermet A.: Assessing the thermodynamics of the Fe-Co-Ni system using a CALPHAD predictive technique, 1989, Calphad, vol. 13, pp. 1-22.

[20] Sundman B., Jansson B. and Andersson J.-O.: The Thermo-Calc databank system, 1985, Calphad, vol. 9, no. 2, pp. 153-190.

[21] Scheil E.: Bemerkungen zur Schichtkristallbildung, Retrograde saturation curves, 1942, Z. Metallkunde, vol. 34, pp. 70-72 (in German).

[22] Gulliver G.H.: The quantitative effect of rapid cooling upon the constitution of binary alloys, 1913, J. Inst. Metals, vol. 9, pp. 120-153.

[23] Wessman S., Pettersson R., Hertzman S.: On phase equilibria in duplex stainless steels, 2010, Steel Res. Int., vol. 81, no. 5, 337-346.

[24] Andersson J.-O., Höglund L., Jönsson B. and Ågren J.: Fundamentals of Ternary Diffusion, Pergamon Press, NY, USA, 1990.

[25] Hillert M.: Phase Equilibria, Phase Diagrams and Phase Transformations, Their Thermodynamic Basis; Cambridge University Press, (1998)

[26] Thier H., Bäumel A. and Schmidtmann E.: Einfluss von Stickstoff auf das Ausscheidungsverhalten des Stahles X5CrNiMo1713, Influence of nitrogen on the precipitation behaviour of steel X5CrNiMo1713, 1969, Arch. Eisenhw., vol. 40, no. 4, pp. 333-339 (in German).

[27] Terada D., Yoshida F., Nakashima H., Abe H. and Kadoya Y.: In-situ Observation of Dislocation Motion and its Mobility in Fe-Mo and Fe-W Solid Solutions at High Temperatures, 2002, ISIJ Int., vol. 42, no. 12, pp. 1546-1552.

[28] Fridberg J., Törndahl L.E. and Hillert M.: Diffsusion in iron, Jernkontorets Annaler, 1969, vol. 153, 263-276.

[29] Nitta H., Yamamoto T., Kanno R., Takasawa K., Iida T., Yamazaki Y., Ogu S. and Iijima Y.: Diffusion of mulybdenum in α-iron, 2002, Acta Mat., vol. 50, pp. 41174125.

[30] Pearson W.B.: A handbook of lattice spacings and structures of metals and alloys, Pergamon Press, 1958.

About the authors

Mr. Sten Wessman (sten.wessman@swerea.se) is with Swerea KIMAB AB (Sweden), Dr. Leif Karlsson (leif.karlsson@esab.se) is with ESAB AB (Sweden), Dr. Rachel Pettersson (rachel.pettersson) is with Outokumpu Stainless AB (Sweden), Dr. Agneta Östberg (agneta.ostberg@sandvik.com) is with AB Sandvik Materials Technology (Sweden).